Dislocations in stripes and lattice Dirac fermions

Mesaroš, A.

Chapter 1

Introduction

In the modern world, the beauty and essence of physics tend to be assigned to the endeavor of finding a single, simplest, and unifying principle describing the root of everything we can observe around us. The champion disciplines of this greedy side of human curiosity are the theories of the extremely small and big (e.g. string theory and cosmology), while the guiding principle of reductionism has been present in modern physics since its birth with Galileo.

However, the very concept of a modern "natural science" is based on Platonic ideas of assigning abstract notions (and therefore quantities) to the plethora of phenomena our senses expose us to. When one approaches the phenomenology of tangible objects which share the space and time scales of human beings, one cannot avoid the amazement when surprising worlds, each with its own rules, populate this window of experience. We expect that the laws of phenomena found in chunks of matter should be set by the nature of its minuscule building blocks, but practically always new laws *emerge* "out of nowhere". The emergent laws, and the belonging *effective theory* can have unexpected forms (symmetries), and lend exciting insight to unrelated systems with same effective theories.

This thesis explores the role of special physical states, *topological defects* (with emphasis on *dislocations*), within several electronic two dimensional condensed matter systems: graphene, topological insulators, and high-T_c cuprates. Since the effective theories of the first two systems mimic fundamental theories (like the fundamental massless fermions, and spaces with gravity), we try to exploit the connection to learn about both sides. On the other hand, these defects are a special kind of disorder because their topology fundamentally destroys the underlying order. We find that topological defects live up to their special role

when two different orderings coexist in the case of cuprates. Additionally to the main subject of defects, we study the effects the electron ordering in cuprates on the lattice phonons. This Introduction therefore starts with a short review of whys & hows of effective theories, continues with a presentation of topological defects and relevant physical systems, finishing with a more detailed motivation and summary of results of the thesis.

1.1 Effective theories

In a few examples, the *effective theory* accurately describing a piece of ceramics (a masterfully cooked one, that is) has tantalizing visualizations in terms of the minuscule, as well as fascinating applications at the same time: from fractionalized electrons to everyday lossless energy transport; In ^{3}He at milliKelvin temperatures, the excitations are effectively described by a theory of fields in gravitational spacetime; In Chapter 2 we will meet graphene described as fundamental fermions in spaces with gravity and torsion; In one dimensional fermion systems, the electron separates into a chargeless spinon, and a spinless holon; The 2D electron systems under high magnetic fields look like they host particles with charge equal to fraction of e. The field of modern condensed matter physics deals with the ever-growing list of such phenomena appearing on scales where it becomes impossible or impractical to describe the system directly through its constituents.

The change of quantity into quality is a fundamental process, as P.W. Anderson succinctly argued through the maxim "More is Different" [1] while defending the elemental nature of modern condensed matter theory. He himself created the famous effective theory of gauge symmetry breaking [2] to explain the superconducting pieces of material in the condensed matter laboratory. The theory is named Anderson-Higgs mechanism, because the high-energy researcher P. Higgs found the same law in the context of the fundamental particles of the electroweak interaction [3]. The effective theories of condensed matter systems can therefore be novel, but also simple and mimicking the fundamental theories of the Universe. To see why this happens, we first have to explore what determines an effective theory.

The *state* of macroscopic matter such as a piece of material, is naturally described by thermodynamic variables like temperature, volume, pressure, magnetization, etc., but its *phase* is characterized by the law that these variables follow. More precisely, Landau identified each phase with the thermodynamic variable — an *order parameter* — that becomes non-zero in the transition to that phase [4]. The equation governing this specific variable, or equivalently the general way in which this variable enters the thermodynamic state function of the system, is classified by its *symmetries*. In the example of magnetic systems, magnetization is a real vector with accompanying $O(3)$ symmetry of real-space rotations; in simple s-wave superconductors, the particle-hole correlator is a complex function

with $U(1)$; and in Chapter 7 we will explicitly construct order parameters to describe the electronic patterns in underdoped cuprates. The concept of local order parameters, naturally seen as fields fluctuating in space and time, is crucial to modern physics. It is important to notice that these fields are inherently classical, as they describe the state of observable macroscopic matter, in contrast to the quantum field operators which are fields describing the exact quantum state of the many-particle system.

We can formally restate the above by saying that the fact that a physical system is able to settle into a ground state (develop a non-vanishing value of the order parameter) that does not respect the symmetry with respect to that order parameter is a consequence of the qualitative transition with size, from quantum mechanical to macroscopic. Suppose the system is prepared in a state with a non-vanishing order parameter. The quantum mechanical dynamics of the macroscopic system is too slow to explore all the other degenerate ground states connected by symmetry transformations, at least on the timescale of measurement. The dynamical time normally scales exponentially with the system size, reaching the lifetime of Universe for a spoonful of particles.

It is important to note that the research of the past decades has shown how sometimes the Landau classification is not exhaustive. Specifically, spin liquids, quantum Hall states, and even insulators and superconductors [5] can exhibit *topological order* [6]. It is based on non-local order parameters while the corresponding effective theory generically is a topological field theory whose states are classified only by global properties of the degrees of freedom. This leads to ground states degeneracies, excitations which acquire phases upon moving around each other, and non-trivial dynamics on the sample edge. These orders are harder to classify and measure, but the systems have inherent robustness to local perturbations, which seems like a lucrative playground for quantum computation applications [7].

Under which circumstances should we expect the (naturally approximate) effective theory to hold? The process of measurement is also characterized by the spatial resolution of the probe, and the amount of energy exchanged. The condition of small energy exchange with the external probe suffices to enter the regime where only collective excitations are visible (and governed by the effective theory), while the microscopic blocks of the system are hidden because there is not enough energy to excite them. The spatial coarse-graining additionally leads to the transition from the discrete to a continuum description. In special cases, near phase transitions, the divergence of characteristic lengthscales and ensuing self-similarity mean that the few degrees of freedom left after coarse-graining very accurately describe the many degrees of freedom present initially. The *renormalization group* theory describes this coarse graining in a process of integrating out small-wavelength fluctuations in the action [8]. The long-range (continuum) limit takes care to correctly describe only the states close to the ground state energy, where "close" is meant in units of the energy of microscopic constituents and their interactions. In other words, usually the energy level

spacing scales like $1/a$, where a is the microscopic lengthscale (e.g. the lattice constant of crystals), ensuring that in the continuum limit where $a \to 0$, the low-energy spectrum is continuous (if not empty), mimicking a true continuum field theory.

It now seems plausible that many microscopic theories converge to the same effective theory (the adiabatic principle), which is set by the dimensionality and symmetry. The high-energy and condensed matter fields therefore both sip from a relatively smaller pool of available field theories.

A field theory however is not a perfect object, and we additionally know it is only an approximation to the condensed matter system behavior. The connection between the (microscopic) high-energy and the (macroscopic) low energy effective theory can sometimes be at a strangely deep level, as in the example of *anomalies*. An anomaly occurs when the symmetry of the (effective) Lagrangian is broken "unexpectedly", by the nature of phase space (measure of the path integral), or through the quantization procedure itself. Here we mean the quantization of effective degrees of freedom. The ensuing non-conservation of a Noether current has a physical interpretation in the interaction of macroscopic and microscopic degrees of freedom. In examples, the charge-conjugation—parity anomaly leads to non-conservation of electric charge in polyacetylene chains and graphene [9,10], under lattice distortions (some charge escapes to the edges of the sample); the chiral anomaly leads to non-conservation of particle momentum in ^{3}He [11], which just means that the momentum is transferred to the anisotropic momentum texture of the liquid. All these are different from the standard mechanism of entropy production by friction, and the forces driving anomalous non-conservation are dissipationless. The fundamental theories of high energy physics do not have the privilege of being connected to a "microscopic" system, so that there anomalies are less amusing.

Before we move on to considering the stability of states described by an effective theory, we finish this Section with the particular example of gravity as an effective theory that is central to Chapter 2 of this thesis. The purpose of this short introduction is to remind the condensed matter physicist (without offering any rigor) of this prime example of a high-energy theory, which she/he probably does not use in everyday work. The goal is also to give some plausibility to its appearance in the context of well-known condensed matter theory of elasticity. A thorough analysis of this subject exists in Ref. [12], and as noted before, gravity also appears in the context of excitations in ^{3}He [11].

1.1.1 Gravity in elasticity

The modern Einstein's theory of gravity is supposed to describe the dynamics of curved spacetimes and matter within it. Because of the curvature, the shortest paths in the space are not straight lines, and particles following them therefore are effectively experiencing (gravitational) forces. Additionally, the gravity equations are the same in any coordinate system, so that accelerating frames of

reference are (in terms of center of mass) indistinguishable from frames moving in gravitational fields, thereby realizing the equivalence principle between inertial and gravitational mass. This requirement means that only intrinsic properties of the curved spacetime (like its local curvature) are physically observable.

All the above properties mean that we can use the tools of differential geometry to describe a spacetime [13], and this is why the connection to elasticity will also appear. The fundamental dynamical variable for spacetime becomes the metric $g_{ij}(\vec{x})$ (for simplicity, we forget time from now on), which gives the local distances (dl) between points:

$$dl^2 = g_{ij}(\vec{x})dx^i dx^j. \tag{1.1}$$

The distance must be invariant to local changes of the coordinate system (and accompanying frames) $x^i \to x^i + \xi^i(\vec{x})$, and that enforces the change:

$$g'_{ij} \to g_{ij} + \nabla_i \xi_j + \nabla_j \xi_i. \tag{1.2}$$

We are free to choose an arbitrary frame at each point $\vec{x}$ (before even considering changing frames), so we a priori need to specify how these frames are related. For a curve C connecting points $\vec{y}$ and $\vec{y}'$ this is done by the rule of *parallel transport* in our space, $\mathcal{P}[C]$, which acts on any physical field (e.g. vectors). We also want this parallel transport rule to be independent of arbitrary frame changes, i.e. to commute with frame changes $dx'^i = \beta^i_j(\vec{x})dx^j$ at each point in space:

$$\mathcal{P}'[C] = \beta^{-1}(\vec{y}')\mathcal{P}[C]\beta(\vec{y}). \tag{1.3}$$

Please notice that we are suppressing the myriad of indices, both related to the action on frames and action on physical fields through a particular representation of $\mathcal{P}$. Locally, when the points $\vec{y}'$ and $\vec{y}$ are close, and $\mathcal{P}[C] \sim \mathbb{1} + \Gamma$, we get the familiar rule defining the behavior of the *connection* Γ:

$$\Gamma' = \beta^{-1}\Gamma\beta + \beta^{-1}d\beta. \tag{1.4}$$

Any familiarity of the transformation rule (1.4) from gauge theory is far from accidental, as gauge theories are also described by differential geometry; it is only that instead of tangential frames, they have spaces with group actions living at each point of space. The connection Γ there just becomes the familiar gauge potential. The natural casting of gravity theory as a gauge theory of "space itself" (i.e. of space translations and rotations) has been a long and tricky pursuit in physics (see [13–15] and references therein; for the condensed matter aspect of the pursuit see [16–18]).

In Einstein's theory the connection becomes the well-known Christoffel symbol Γ^i_{jk}, which is completely determined by the metric field g_{ij}, because it is also demanded that parallel transport does not change lengths of vectors it transports. Arbitrary *curvature* can be accommodated in this theory, because the curvature

is just the field strength belonging to the (non-Abelian) "gauge potential" Γ:

$$R = d\Gamma + \frac{1}{2}[\Gamma, \Gamma]. \tag{1.5}$$

The Abelian version of field strength is well known from electrodynamics. There the connection is the electromagnetic gauge potential $\Gamma \equiv A$, so that $F = dA$, i.e. $F_{ij} = \nabla_i A_j - \nabla_j A_i$. (Because of their visual simplicity and powerful properties, we use differential forms throughout this thesis — a nice tutorial can be found in e.g. [13].)

Torsion

Another crucial assumption is made in Einstein's theory: Loops made by transporting two small vectors along each other are always closed. This corresponds to the symmetry $\Gamma^i_{jk} = \Gamma^i_{kj}$ of the connection. As will be further clarified in Section 1.2.2, this assumption is actually very important, because it needs to be relaxed in crystals by upgrading to Einstein-Cartan (EC) theory (this happens in Chapter 2). The upgrade consists of a new degree of freedom, the *torsion* T, which exactly measures the asymmetry of Γ:

$$T^k_{ij} = \frac{1}{2}\left(\Gamma^k_{ij} - \Gamma^k_{ji}\right). \tag{1.6}$$

We can see the essence of torsion at work by explicitly transporting two infinitesimal vectors a and b along each other, obtaining the vectors $\overline{a}, \overline{b}$, in an attempt to make a closed loop, cf. Fig. 1.1. The law of parallel transport says:

$$\Delta a^i = \overline{a}^i - a^i = -\Gamma^i_{jk} b^j a^k \tag{1.7}$$

$$\Delta b^i = \overline{b}^i - b^i = -\Gamma^i_{jk} a^j b^k. \tag{1.8}$$

The resulting non-closure of the loop, which is called a Burgers vector in crystals,

$$\Delta a^i - \Delta b^i = (\overline{a}^i + b^i) - (\overline{b}^i + a^i) = -T^i_{jk} ds^{jk}, \tag{1.9}$$

is really proportional to the local value of torsion, and the infinitesimal surface spanned by the loop, ds^{jk}. Torsion is a less familiar aspect of the geometrical formulation of gravity [12, 13, 19, 20], because it was ignored at first by Einstein. Cartan [21] advertised it as an *a priori* ingredient of a geometrical theory. It was later pointed out by Kibble [20] that its inclusion becomes necessary in the presence of spinning particles, as their spin currents source torsion in a dynamical space-time. Whether torsion propagates in the space-time is a matter to be settled by observation: so far torsional effects seem to be too weak to be measured.

The relevance of all the above to crystals of condensed matter physics begins by noticing that elasticity theory is based on measuring the energy contribution

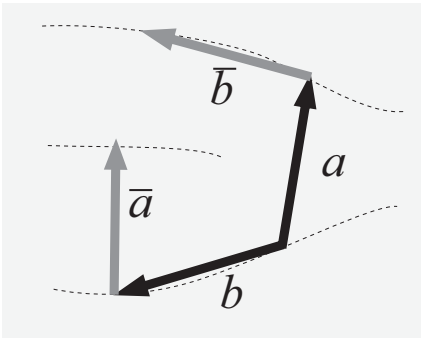

Figure 1.1: Torsion locally measures the non-closure of loops. The vectors $\overline{a}, \overline{b}$ are obtained by parallel transport of a, b along each other. The dashed lines represent the imagined "dislocation" (compare to Fig. 1.4)

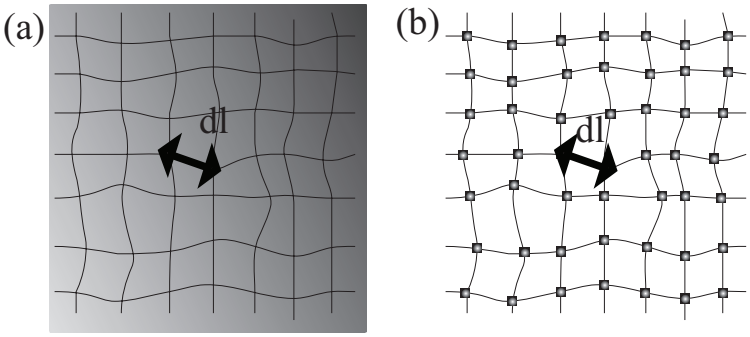

Figure 1.2: Why gravity appears in elasticity. (a) The metric of gravitational spacetimes acts as a local ruler. The system is invariant to arbitrary changes of coordinates in the continuum space. (b) The strain field is a local measure of distance changes in the discrete lattice. Arbitrary displacements cost energy.

from the local strain field. The displacement of atoms causing the strain however is a just a local change of distances (Fig. 1.2). Indeed, the expansion of energy in strains is based on considering local changes of atom distances:

$$dl'^2 - dl^2 = (\nabla_i u_j + \nabla_j u_i) dx^i dx^j. \tag{1.10}$$

This allows us to immediately identify the continuum metric that belongs to the displaced lattice, at least on the level of linearized gravity,

$$g_{ij} = \delta_{ij} + \nabla_i u_j + \nabla_j u_i. \tag{1.11}$$

The deep geometrical content of elasticity is lying in the fact that the crystal displacement $\vec{u}(\vec{x})$ can generate a non-trivial geometry from the ideal lattice. This

happens exactly in cases when crystal contains topological defects (introduced in detail in Section 1.2.2), and is the reason we are studying the elasticity/gravity connection in Chapter 2 of this thesis. To see why defects are the key, we quote the connection generated by the displacement in Eq. (1.11):

$$\Gamma_{ijk} = \nabla_i \nabla_j u_k. \tag{1.12}$$

This carries zero curvature, according to Eq. (1.5), but *only if* the local rotation field $\nabla_i u_j - \nabla_j u_i$ is integrable (not multivalued). Similarly, when the displacement field u_i itself is multivalued, torsion is generated in the lattice. Such non-integrable fields appear automatically in presence of topological defects, as we will see in Section 1.2.2.

The parallel transport picture also follows for physical fields that are tied to the positions of atoms, e.g. the description of electrons through tight-binding [22–25].

The gravity/elasticity correspondence should be thought of as both incomplete and useful. Firstly, the local change of frames generated by displacements is not a symmetry of elasticity, as it costs energy. We must therefore consider gravity in a "fixed frame", a common practice in analogous systems. Secondly, the crystal inherently breaks translations and rotations to discrete subgroups, which means that curvature and torsion are quantized. We can set them to arbitrary values by making them infinitesimal in the continuum description of the crystal. One can nonetheless still study the transport of matter in such non-trivial fixed frame backgrounds: several such analogous gravity systems have been identified, including the sound waves of superfluid ^{4}He and the nodal Fermions of the ^{3}He-A phase, which perceive the hydrodynamical flow fields as geometrical (Christoffel) connection [11]. On the other hand, the crystal picture easily uncovers a richer and less constrained geometry, as in the example of liquid crystal phases [26], or indeed through the presence of observable torsion (which will be the subject of Chapter 2).

After this glance at gravity in condensed matter, we are returning to the general consideration of effective theories. Since we introduced effective theories as describing the low energy behavior of the system which is typically characterized by some ordering, i.e. a broken symmetry, it is just natural that we consider the destruction of that ordering. For this we need to think about general topological defects, especially since our appetite has been opened by their brief appearance in this subsection.

1.2 Topological defects

Whether in a given state our system will exhibit a certain non-zero order parameter, depends on the amount of fluctuations this order parameter is experiencing. The quantum fluctuations decide the ground state at zero temperature, but can also be dominant at finite temperatures [27]. These fluctuations are controlled by

the coupling constants of the theory, including the case of competition between several different order parameters.

On the other hand, thermal fluctuations represent the entropic disordering and lead to well-known classical thermodynamic phase transitions. When the system has a continuous spectrum starting from the ground state energy (i.e., has no gap, or mass), thermal excitation of states of infinitesimal energy can destroy the order and shift the system to a different ground state. This mechanism is ubiquitous since according to Goldstone's theorem the breaking of a continuous symmetry is accompanied by a gapless spectrum (i.e. massless modes). (The standard theories with broken continuous gauge symmetry, e.g. superconductivity, are actually approximate low energy descriptions, so they are allowed to violate both this theorem, and Elitzur's theorem on exactness of gauge symmetry.)

Among all the configurations representing excited states that get mixed with the ordered configuration as the order parameter fluctuates, *topological defects* [28] have a special status, and this section is devoted to them.

Let us start by considering the lowest energy configurations of a system governed by a connected continuous symmetry group G, of dimension n. A state of the system is described by the field $\Psi(\vec{r})$. The symmetry ensures that there is an n-dimensional degenerate manifold $\hat{g}(\vartheta_1, \ldots, \vartheta_n)\Psi(\vec{r})$, explored by generating group transformations along the n group generators $\mathcal{A}_i$, i.e.

$$\hat{g}(\{\vartheta\}) = \exp\,(\sum_i \vartheta_i \mathcal{A}_i), \tag{1.13}$$

with $\hat{g}$ representation of $g \in G$. (We do not consider changes in the order parameter amplitude yet.) If our theory (with fixed temperature and coupling constants) describes the symmetry broken phase, the ground state Ψ_0 is constant in space, and there is a degenerate zero energy manifold M containing all the states $\hat{g}(\vartheta_1, \ldots, \vartheta_n)\Psi_0$. There are n excited modes (Goldstone bosons), in the form of smooth local deformations of the ground state along the i-th direction, $\hat{g}(\vartheta_i(\vec{r}))\Psi_0$, where locality is enforced by demanding

$$\hat{g}(\vartheta_i(\vec{r})) \xrightarrow{|\vec{r}|\to\infty} \mathbb{1}, \tag{1.14}$$

i.e. the Ψ_0 is recovered everywhere in spatial infinity. Goldstone modes have arbitrarily low energy, because the modulation $\vartheta_i(\vec{r})$ can be of arbitrarily long wavelength.

When the system order Ψ_0 survives the smooth Goldstone fluctuations, we must analyze the topological excitations $\Psi_{\rm top}$. These are *non-local* and characterized by taking the $\hat{g}(\vartheta_i(\vec{r}))\Psi_0$ configuration to different zero energy states at different directions $\hat{\vec{r}}$ of spatial infinity, i.e.

$$\hat{g}(\vec{r}) \xrightarrow{\vec{r}\to\infty} \hat{g}(\{\vartheta\}(\hat{\vec{r}})), \tag{1.15}$$

in a non-trivial way. By non-trivial it is meant that the no matter how we locally modulate $\Psi_{\rm top}$ (put Goldstone modes on top of it), or if we apply global transformations $\hat{g}\Psi_{\rm top}$, still the $\Psi_{\rm top}$ will explore a finite portion of M at spatial infinity. A topological defect is therefore special because it truly acts as a disorder operator for the symmetry broken order: the system's preferred choice of Ψ_0 is compromised by taking it through its equivalent, symmetry related, states in M at spatial infinity. Even stronger, the topology ensures that in $\Psi_{\rm top}$ the ordering Ψ_0 will vanish at some points in the system: as we follow inwards from spatial infinity the configurations $\hat{g}(\{\vartheta\}(\hat{\vec{r}}))$, the smoothness of $\Psi_{\rm top}$ ensures that we will reach a region of infinitesimal volume inside the system, *the core of the defect*, where an entire set of configurations from M must coexist. This actually means that the order parameter vanishes at the core.

Topological defects are abundant in condensed matter systems, and some of them will be central to this thesis. In one dimensional systems one can have domain walls in e.g. Ising spin chains and dimerized chains [29]; in higher dimensions there are a variety of dislocations and disclinations in crystals and liquid crystals, vortices in superfluids and planar magnetic models, magnetic vortices in type II superconductors, and a zoo of defects in the complex ordering of ^3He. These defects are of course also relevant for all dual models of these paradigmatic ones. A notable exception to this framework is a skyrmion defect, observed recently in $2d$ magnets without inversion symmetry [30,31], where the topologically non-trivial mapping is from the order parameter space to the sphere which represents the compactified plane (not the spatial infinity).

The energy of $\Psi_{\rm top}$ will typically be infinite (extensive with system size); but defect—anti-defect pairs can always form, where anti-defect $\hat{g}(\vec{r})^{-1}\Psi_0$ cancels the long distance field configuration of the defect. This provides for the concrete possibility of destroying order through proliferation and unbinding of topological defect-pairs. The $2dXY$ model describing thin film superfluids does not have a normal phase transition because its symmetry is continuous ($U(1)$); however a finite temperature vortex unbinding transition was discovered by Berezinskii, Kosterlitz and Thouless [32], where the superfluid phase has quasi—long-range order (power law correlations) below, and disorder (exponential correlation falloff) above the transition temperature [33]. The same mechanism was applied to dislocation mediated melting of crystals [12,34,35], notably leading to a hexatic phase in $2d$. Beyond their energetics, defects interact through their long-range smooth configurations. Additionally, since they might be represented by non-Abelian group transformations, their mutual interactions might not be treatable. In particular, disclination mediated melting, based on destruction of rotational ordering is intractable [12].

The word "topological" is used extensively in this Section because $\Psi_{\rm top}$ is characterized by the mappings of the order parameter space M (or the group representation $\hat{G}$) onto the spatial infinity, modulo all local smooth deformations. For a point topological defect, the spatial infinity is represented by the $d-1$ dimensional sphere S^{d-1} in d dimensions, and all the mappings are classi-

fied by the homotopy group $\pi_{d-1}(\hat{G})$, etc. The language of homotopy theory and group theory in the context of order parameters and defects was interpreted and compiled for physicists by N. D. Mermin [36]. The article came at the end of seventies, a decade in which non-perturbative and topological aspects of (quantum) field theory became intensively studied [37]. It was shown that topological excitations may carry sharp, and even fractional, quantum numbers [38]. Analogously, in gauge theory it was found that topologically non-trivial fiber bundles describe special physical states like the Dirac monopoles of electrodynamics [39]. Considering also the time dimension, topologically non-trivial *instanton* solutions can describe tunneling effects between the ground states. In non-Abelian gauge theories, such topologically non-trivial solutions of finite energy [40, 41] were shown to lead to quark confinement [42, 43].

We will now focus on introducing topological defects which are relevant for the rest of this thesis.

1.2.1 Vortex

A simple condensed matter physics demonstration of the principles described in this Section can be found in the $2dXY$ model. We will encounter them in a slightly modified interpretation as stripe dislocations in Chapter 7. The $2dXY$ model represents two-dimensional magnetic moments (spins) $\vec{n} = (\cos(\varphi), \sin(\varphi)) \equiv \hat{n} = \vec{n}_x + i\vec{n}_y$ in two dimensions, with potential energy on the lattice $V = J\sum_{<i,j>} \vec{n}_i \cdot \vec{n}_j$ (J is an energy scale, and we do not need kinetic energy or quantum mechanics here). In the continuum limit,

$$V = \frac{J}{2} \int \mathrm{d}^2\vec{r} \, \left(\hat{n}^* \vec{\nabla} \hat{n}\right)^2 = \frac{J}{2} \int \mathrm{d}^2\vec{r} \, \left(\vec{\nabla}\varphi\right)^2 . \tag{1.16}$$

The symmetry of the potential are global rotations of $\vec{n}(\vec{r})$ (group $SO(2)$). In the language of the angle $\varphi(\vec{r})$, the group is $U(1) \simeq SO(2)$, with transformations $\varphi \to \varphi + u$, and the model describes the phase fluctuations of a superfluid. The ground state is given by a constant phase $\varphi(\vec{r}) = \varphi_0$. The topological defects (*vortices*) are classified by elements of $\pi_1(U(1)) \simeq \mathbb{Z}$. The integer class of a vortex, its *topological charge* called "vorticity", $n \in \mathbb{Z}$ is

$$n = \frac{1}{2\pi} \oint_C \mathrm{d}\vec{r} \cdot \vec{\nabla}\varphi(\vec{r}) \tag{1.17}$$

equal to the winding number, telling how many times the vector $\vec{n}$ rotates a full circle in the counter-clockwise direction, as we follow an arbitrary path C around the defect. All these paths are topologically equivalent to a circle at spatial infinity, and n does not depend on their shape or size. The vortex with winding number n must contain the topologically non-trivial multivalued [44] configuration $\varphi^{\mathrm{v}}(\vec{r}) = n\theta$, where θ is the polar angle, Fig. 1.3. (The superfluid wavefunction stays singlevalued when its phase jumps by multiples of 2π.) A

global rotation by $-\pi/2$ creates the equivalent "hedgehog" profile. The field is undefined at the origin (defect core); the order parameter is actually suppressed to distance a_c from the origin, defining the physical defect core size, which is of order the short-distance cutoff (lattice constant).

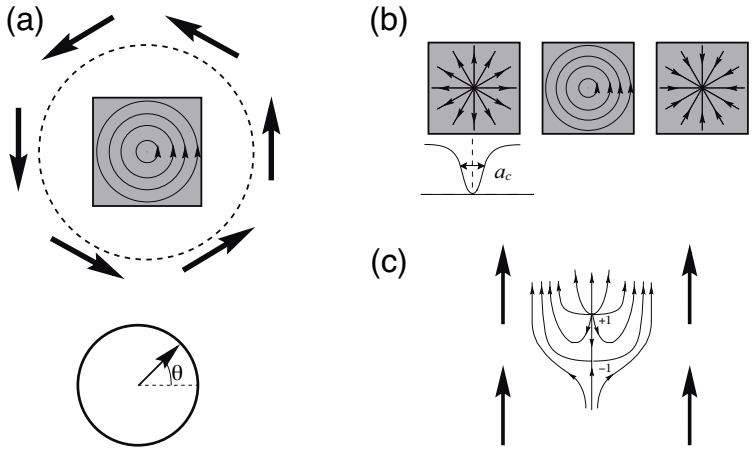

Figure 1.3: The vortex of the $2dXY$ model. (a) At infinity the vector winds one full circle, $n = 1$, following the polar coordinate. (b) Three equivalent representations of $n = 1$ vortex, obtained by global rotations (no energy cost). The vector vanishes in core region of size a_c. (c) Topological charge n is additive: here $n = 1$ and $n = -1$ cancel at infinity.

The energy of the vortex configuration is diverging with system size L: $V_{\rm v} = J\pi \ln(L/a_c)$. To understand this, observe that the local contribution to the potential energy from $\varphi^{\rm v}(\vec{r})$ is determined by $|\vec{\nabla}\varphi^{\rm v}| \sim 1/r$; on the other hand, a low energy Goldstone mode (a plane wave) would have wavelength of order inverse system size $1/L$, with local energy given by $|\vec{\nabla}\varphi| \sim 1/L$. This shows that the long-range effect of $\varphi^{\rm v}(\vec{r})$, needed to ensure the topological property at all distances, is responsible for the diverging $\ln(L)$ term.

When multiple vortices are present, the model maps to the strictly $2d$ Coulomb gas, with vortices acting as points of charge n, and the force mediated by the smooth field deformations [45].

1.2.2 Crystal dislocations

Crystal lattice dislocations will be of central interest to most of this thesis, while the crystalline order itself is the most fundamental one of solid state physics. It breaks the translational and rotational symmetries of a gas (or liquid). In real crystals obviously there are many imperfections: vacancies and interstitials (these are point defects), dislocations and disclinations (line defects in $3d$, but

point in $2d$), grain boundaries (planar defects, line in $2d$). The point defects are energetically very costly, but certainly important for electronic behavior of crystals. However, they only change the number of atoms participating in the crystal order, and lack the non-local effect at spatial infinity. We will visit grain boundaries in detail in Chapter 4. This subsection is devoted to the topological defects concerned with restoration of translational and rotational symmetry breaking: dislocations and disclinations, respectively, with focus on the former. For all historical developments mentioned here, please see the personal recollection in Ref. [46] and references within it.

An essential understanding of crystal defects comes from the Volterra construction, devised a hundred years ago. His idea was that some internal stresses in the material come from a relative misalignment of crystal pieces within it. He imagined "cutting" into the crystal along a surface, performing a relative misalignment in the two loose pieces — by displacement or some twisting — and then "gluing" back the pieces. Because the operation performed is a symmetry operation of the given crystal, the pieces fit back together on the entire "Volterra cut" (surface) except at the line marking the edge of the surface inside the crystal (there the operation was ill-defined). This line is the defect (core) line as we know it today [47]. The choice of the position and shape of the Volterra surface is actually a gauge freedom on its own [12].

Weingarten took this construction a step further by considering the strain and rotation fields, i.e. the symmetrized and antisymmetrized derivatives of the displacement field $\vec{u}(\vec{r})$ in the crystal. The former are physical fields, in contrast to the $\vec{u}(\vec{r})$ which suffers from ambiguity — crystal is periodic, so from which ideal atom position do we measure the displacement of the real atom? (This ambiguity can actually be cast in the form of a gauge degree of freedom [12].) He then found that the discontinuity of $\vec{u}(\vec{r})$ upon encircling a defect line along an arbitrary path C (one can heuristically imagine the jump occurring on the Volterra surface):

$$\oint_C \left(\mathrm{d}x \cdot \vec{\nabla}\right) \vec{u} = \vec{b}_0 + \vec{\Omega} \times (\vec{r} - \vec{r}_0), \tag{1.18}$$

with $\vec{r}_0$ a reference point and $\vec{r}$ the point to which we are assigning the jump in $\vec{u}(\vec{r})$. The conclusion is that all topological defects are exhausted by ones performing displacements and rotations in the Volterra construction. Purely translational defects are dislocations, having $\vec{\Omega} = 0$, and the *Burgers vector* $\vec{b}$. This vector can at any point be at arbitrary orientations to the defect line in $3d$. In $2d$ the defect core is a point representing a section of the defect line running along the third coordinate, while $\vec{b}$ lies in the $2d$ plane — therefore all dislocations are of "edge" type. The Frank vector $\vec{\Omega}$ represents a rotational action; in $2d$ it becomes a scalar Ω because only rotations around the third coordinate are possible in the $2d$ plane.

The essential geometric property we can see in the topological behavior of Eq. (1.18), is that the displacement field $\vec{u}\vec{r}$ becomes non-integrable when there

are dislocations present. This is the type of geometric property that identified these crystal defects as crucial in the mapping of crystal elasticity to fixed-frame gravity in Section 1.1.1.

An example of a dislocation in a square lattice is shown in Fig. 1.4. The half-line of missing (or added) atoms is along the Volterra cut, and represents the translation operation by one lattice constant. This operation leads to the Burgers vector $\vec{b}$ of that exact length.

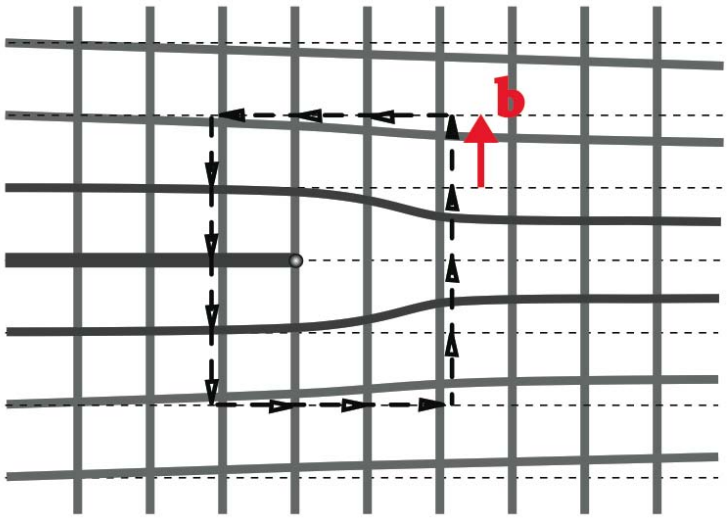

Figure 1.4: Dislocation in a square lattice. The ideal lattice is in dashed lines. The missing half-row at the Volterra cut produces a "missing step" along the Burgers vector $\vec{b}$, of length one lattice constant. The "step" persists for any contour enclosing the defect.

One might want to be convinced about the topological nature of these defects through a construction along the lines introduced earlier in this Section [48]. The construction is not as straightforward as one would wish, because the order parameter should describe the position, orientation and shape of unit-cells — this information is not really contained in a point of space, as is true for spatially uniform systems. If we treat such problems in a cavalier manner [36], we can at least say that the displacement field $\vec{u}(\vec{r})$ is the order parameter describing any state of the crystal. The vector is periodic at each point in space (for each atom), because it does not matter from which ideal lattice position we want to measure the position of the atom [49]. The order parameter $\vec{u}$ therefore occupies the surface of a torus. Following the loop around the dislocation also produces a loop around the torus (along the radius of the torus representing the $\vec{b}$ direction). The winding number around a radius of the torus is the measure of length of $\vec{b}$

in the corresponding direction.

Luckily, the strict topological description was not necessary for the historical recognition of dislocations and their role in crystals. The name "Burgers vector" comes from J. M. Burgers who first correctly realized the need to assign the vectorial quantity to this particular type of defects. His realization came in 1930s, while theories trying to use defects to explain material properties were ripe. Dislocations reduce the shear modulus of crystals, which would be huge thanks to strong interatomic forces, by several orders of magnitude. Namely, a small (energetically attainable) rearrangement at the defect core can severe a connection between two atom half-lines, match one of them to the half-line of "Volterra added atoms", and pronounce the orphaned half-line the "intruder". The crystal can make a dislocation—anti-dislocation pair, and propagate shear stress by letting them move in opposite directions. Another crucial effect is work hardening, whereby repeated shearing of a material produces a tangle of dislocation defect lines. The elastic stress of this tangle prohibits new defect formation, and the shear modulus becomes prohibitive, as in an ideal crystal.

Finally, it is interesting to note that all the types of crystal defects are not entirely independent. A disclination dipole forms a dislocation, and a stack of dislocations can form a disclination. The reason for this interrelation lies deeply in the intricacy of the Euclid group (the group of all rotations and translations of space). Here we only point out the crucial fact that rotations and translations become indistinguishable when considered as local (space dependent) operations [50]. Another connection between defects is that a line of parallel dislocations forms a grain boundary: This fact will be important for us in Chapter 4.

1.3 Physical systems studied in this thesis

We devote this Section to a very brief review of three types of physical systems that are studied in this thesis. All are two-dimensional, but differ in essential aspects: While graphene and topological insulators are here studied primarily in the context of non-interacting low energy behavior, the high-T_c cuprates we deal with in Chapters 6, 7 are crucially a strongly correlated electronic system. The first two share the aspect of massless fermionic excitations, while in the last one we analyze an effective theory of bosonic order parameter fields.

In Chapters 2, 3, 4 of this thesis, the influence of crystalline defects on electrons of graphene is studied through the low energy continuum theory in conjuction with numerical tight-binding modeling. In Chapter 4 we relate to recent scanning tunneling microscopy (STM) experiments, while in Chapter 3 we analyze a hypothetical mesoscopic transport interference experiment. Chapter 5 describes dislocation effects in a class of topological insulators, using a mesoscopic interferometer with a simple (not yet built) design. In Chapter 6 we switch to the high-T_c cuprates, studying the electron-phonon coupling dominated by electronic stripe order directly connected to the scattering measurements of phonon

anomalies. Finally, in Chapter 7, our coupled order parameter theory is directly based on the analysis and interpretation of STM studies of several underdoped high-T_c cuprates. We expect that the insights about relative importance and interplay of order parameters, as well as the uncovered novel characteristic effects, will pertain to generic cuprate systems.

1.3.1 Graphene

Graphene is a two-dimensional, one atom thick, carbon atom honeycomb lattice, which was amazingly made for the first time less than a decade ago, by a direct extraction from graphite of a pencil [51]. Just being a real two dimensional sheet makes graphene an exceptional material; additional properties make it a very rich system with huge potentials. In this subsection we can only present a very subjective review of selected research done on graphene in the past decade; the reader is referred to recent reviews [52,53] for a guide to the extensive literature.

The 2*d* graphene "crystal" (a big molecule reaching tens of microns) is now being produced comfortably, both on substrates (through exfoliation and epitaxial growth) [54], and in the form of a standalone sheet [55]. Even in the former case, graphene *per se* is observable thanks to the achieved degrees of decoupling from the substrate [56,57]. The mechanical properties of the graphene sheet are superb, but its electronic state has been a real gold mine so far.

Almost five decades ago, it was shown [58] that the triangular lattice symmetry, together with a two-atom crystal unit-cell (two Bravais sublattices A/B), must lead to a massless Dirac spectrum (see Fig. 1.5).

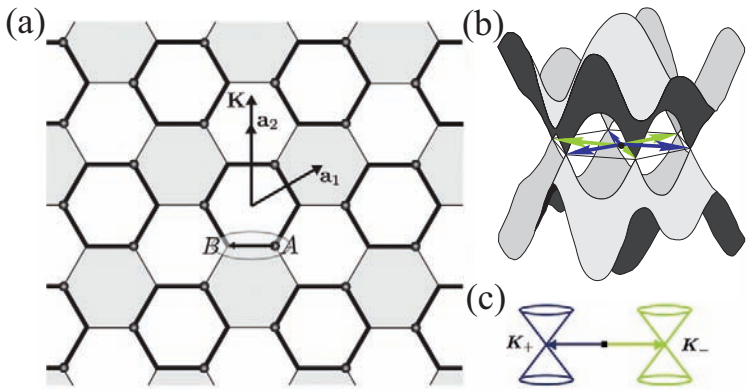

Figure 1.5: Dirac fermions in graphene. (a) The honeycomb latttice has two atoms (A/B) in the unit cell. (b) The tight binding spectrum, with two inequivalent Fermi points at opposite momenta $K_\pm = \pm K$. (c) The low energy Dirac cones are protected by the lattice symmetry. The A/B sublattice plays the role of spin of Dirac particles.

The low energy theory does take the form of a Dirac equation, with two important differences: (i) the fundamental Dirac spin is replaced by the sublattice A/B (the real spin of graphene becomes a separate intrinsic degree of freedom); and (ii) there are two species of Dirac particles, because there are two Dirac cones: one for each Fermi point $K_\pm$ (these two species are called also "valleys"). The continuum Hamiltonian is (σ act on sublattice space):

$$H = -i\vec{\sigma} \cdot \vec{\nabla} \,. \tag{1.19}$$

Starting from this fact, the peculiar Dirac particles with their massless linear spectrum lead to many essential physical differences from the standard massive band electrons. Many of these have been demonstrated experimentally already: the Klein tunneling [59], anomalous Hall effect [60], optical absorption set by the fine structure constant [61], peculiar plasmon modes [62], etc. All these behaviors are consequences of behavior of fundamental Dirac particles in presence of interactions and coupling to electrodynamics. In Chapter 4 of this thesis we also find that the presence of crystal defects allows the measurement of Dirac zero modes, which indicate the anomalies of the Dirac theory. All this also means that converse is true: graphene represents a laboratory for the high-energy fundamental theory of spinful particles with quantum electrodynamics. Due to the correspondence between elasticity and gravity (which is carried through by crystal defects, see Sections 1.1.1, 1.2.2), graphene is also a laboratory for the coupling of spinful particles to non-flat, gravitating, spaces. The Chapter 2 of this thesis is devoted to just such effects.

The above theoretical delights created the initial excitement about graphene. Along the way, it is proving even more versatile in practical applications [52], and we want to close this subsection by mentioning a few of our favorite recent advances. The superb electron mobility of graphene indicates electronics applications (i.e. the new generation of transistors). This pends on the, much sought for, control of a gap in the graphene spectrum, which is becoming a reality through fabrication [63]. Secondly, a novel type of spintronics awaits the precise control of the valley degree of freedom [64]. Finally, the thinness and conductivity of graphene have been shown to allow for efficient screening of each base in a single DNA molecule which is driven through a hole in the graphene sheet [65], therefore opening the scene for fast and complete individual DNA sequencing.

1.3.2 Topological insulators

It might seem at first that all insulators all the same — once there is a gap in the bandstructure, and no low lying states near the Fermi level, there is not much to say. In the past decade it turned out that an elegant classification of different phases of insulating matter exists. This classification is achieved through topological invariants, and cannot be expressed through the Landau symmetry breaking paradigm. Additionally, the novel states bring excitement because they lead to potentially useful applications.

A simple way to see that not all insulators have to be the same, is to realize that there are many topological field theories that might just describe a physical system. These field theories only measure some topological invariant of the system, and the physical spectrum has a gap. The simplest relevant example for us is the Quantum Hall Effect (QHE) which occurs in a two dimensional electron gas under high magnetic fields [66]. The corresponding field theory for one Landau level is the Chern-Simons action [67]:

$$S = \frac{1}{4\pi\nu} \int \mathrm{d}^2\vec{r}\mathrm{d}t \; a\mathrm{d}a, \tag{1.20}$$

where $a = a_\mu \mathrm{d}x^\mu$ is a fictitious gauge field. This action has no dynamics in the bulk, but there is an analogue of the Goldstone bosons of the usual field theories! Namely, when the system has a boundary, the action S describes a gapless state living on the boundary. This state gives the quantized Hall conductance $\sigma_{xy} = Ce^2/h$, with $C = \nu$ (see [68] and references therein).

In the Integer QHE regarded so far, $\nu = 1$ for the single Landau level. However, all relations pertain also to the "Laughlin" Fractional QH states with $1/\nu$ an odd integer, which appear in cleaner samples and higher fields [69]. There the underlying physics is very different [70], while the resulting field theory are the same, in the spirit of our discussion at the beginning of this thesis.

Going back to IQHE, but now with n filled Landau levels, the conductance is quantized with $C = n$. This fact follows actually from the topological nature of the number C. It is equal to the number of times the phase of the many-body wavefunction $|\psi_{\vec{k}}\rangle$ wraps around the (periodic) Brillouin zone (BZ) — the TKNN number [68]. The Berry connection describing the transport of the phase (which is a $U(1)$ degree of freedom), is given by $A(\vec{k}) = \langle\psi_{\vec{k}}|\nabla_{\vec{k}}|\psi_{\vec{k}}\rangle$, and its field strength $F = \mathrm{d}A$ determines the "Chern" number C:

$$C = \frac{i}{2\pi} \int\limits_{BZ} F = \frac{i}{2\pi} \int\limits_{BZ} \mathrm{d}^2\vec{k} \nabla_{\vec{k}} \times A(\vec{k}). \tag{1.21}$$

This invariant, and the entire classification, can be generalized to systems with interactions and disorder by considering the many particle wavefunction with twisted boundary conditions in real space [28, 71, 72].

The topological insulators are states of matter analogous to this IQHE example; they however do not have a magnetic field present, so that time reversal is an additional symmetry. A topological classification of Bloch Hamiltonians living on the Brillouin zone (analogous to the above classification of wavefunctions), including the time reversal symmetry, gives a $\mathbb{Z}_2$ classification [73]. The even/odd topological invariant $\mathbb{Z}_2$ counts whether there are even or odd number of time reversed mode pairs on the edge of the system, and is a direct proof that non-trivial topological insulator states without magnetic field could arise [74]. A realization of a non-trivial topological phase ("odd") was found in the model of

graphene with spin-orbit coupling [75], although unfortunately this coupling is not large enough in real graphene.

The importance of spin-orbit coupling for realizing the non-trivial topological states of insulators was actually uncovered earlier. The deep connection was found when the QHE was generalized to four dimensions: there the Hall current carried by the edge states was replaced by a dissipationless spin current [76]. Coming back down to three dimensions, a realization of such spin currents driven by an electric field was predicted and found in semiconductors with spin-orbit coupling [77–80]. The voltage driven dissipationless spin current in a charge insulator would be crucially important for spintronics applications. In our present context, the discovery is of the new phase of insulating matter, with a topological protection. The quantization of the non-zero spin conductance in two dimensions could occur when lattice strain induces a Landau level type discretization of the spectrum [81], making the analogy with the QHE direct: The spin-orbit coupling behaves as an effective magnetic field of opposite sign for the two spin directions, and thereby the system is two copies of the QHE Eq. (1.20) with opposite chiralities of edge states. The topological insulators can therefore exhibit the Quantum Spin Hall (QSH) effect, with non-vanishing spin Hall conductance (the normal QHE is not present, $\sigma_{xy} = 0$): there are protected pairs of helical modes on the edge, each partner in the pair carrying the opposite spin in opposite direction.

Remarkably, the initial considerations of spin-orbit coupling effects allowed for direct predictions of materials that should exhibit the topological states, and two dimensional realizations followed [82, 83].

The consideration of higher dimensional topological insulators brings additional surprises. A complete classification of topologically non-trivial insulating phases of non-interacting matter (where the gap is of arbitrary origin, e.g. superconductors) was achieved by considering the classification of topological field theories and their propagating edge states [84, 85]. There are five classes of topological insulators in every dimension, and all are further labeled by a $\mathbb{Z}$ or $\mathbb{Z}_2$ invariant. These invariants determine the physical properties of the states, including the modes on the boundary. It turns out that in three dimensions a topological insulator can host a surface mode which is a single Dirac particle. This is in contrast to the fundamental Nielsen-Ninomiya theorem [86] which demands fermion doubling in lattices: The sidestep is allowed because the system exists only as a boundary of a lattice. Striking experimental realizations have put the possibility on firm footing [87–89]. Such helical Dirac particles are even more peculiar than their paired versions occurring in e.g. graphene (Section 1.3.1). We will study their interaction with topological defects in Section 5 of this thesis.

1.3.3 The high-T_c cuprates

Since their accidental discovery [90], the high-T_c cuprates ("cuprates") have been generating an immense amount of research. One line of motivation for this effort

is the direct value for society (and backreaction on physics), embodied in perfecting and controlling ever-more robust materials with ever-higher T_c's. The success in this area has been limited in view of the invested effort, maybe primarily because of the very hard challenge of making real progress along the second line of motivation — which is the understanding of physics of these materials. The hard nature of this challenge is tied to the fact that the electrons in cuprates are strongly correlated, and the nature of resulting system excitations is not obvious.

The electrons are active in $2d$ perovskite planes (with a CuO_2 unit-cell). The parent compounds have one hole per unit-cell, but are not metallic at all: Instead they are antiferromagnetic insulators. These are understood as Mott insulators, states where the strong Coulomb repulsion of electrons leads to localization of charge. The microscopic Hubbard model for fermions at half filling catches this physics well, and leads perturbatively to the effective low-energy theory which involves only spin. The coupling is antiferromagnetic because of virtual excitations of double occupancies. The strong interactions are therefore under control through the effective theory.

Upon forcing charge double occupancies through chemical doping of the parent compound, the system exhibits perplexing complexity with universal features shown in Fig. 1.6. The well controlled extreme corner of the phase diagram (the antiferromagnetic insulator) only survives for very low dopings. At optimal dopings, the normal phase which competes with superconductivity is the "strange metal" (i. e. not a Fermi liquid), a state exhibiting some signatures of criticality. At lower than optimal dopings ("underdoped") there is the similarly unusual "pseudogap" phase. It is not a superconducting state, but its spectrum has a gap of an uncertain origin. At the other extreme, the highest dopings, the large density of holes allows for the familiar Fermi liquid.

The standard BCS superconductor theory [91], which treats a perturbed Fermi liquid, is obviously far off the mark. The defining property of a high T_c value is determined by what the system is trying to do when it is not a superconductor. The challenge is to identify the relevant degrees of freedom and build an effective theory (and/or a microscopic model) that reproduces the phase diagram. It is therefore crucial to identify which symmetries are broken and how. The shape of the transition lines in the phase diagram is suggestive of a (maybe not single) quantum phase transition hidden below the superconducting dome. That would be nice for theorists, and again suggests focusing on a minimal set of order parameters determining the ground state at zero temperature. As an example of the many contenders for "The" high-T_c theory, we want to mention the early, long standing RVB theory [92], whose ansatz ground state consists of singlet pairs with the Mott insulator charge occupancy restriction.

Unfortunately, the strongly correlated systems might exhibit orderings which are not crucial for the underlying novel physics. The intellectual battle for determining the status and role of such orders is the best driving force for experiments. So far, experiments on cuprates convincingly show that the pseudogap phase is characterized by breaking of crystal lattice symmetries.

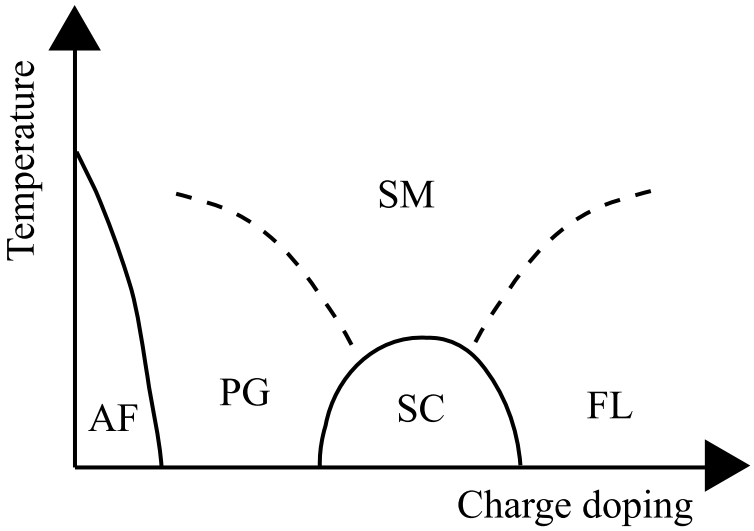

Figure 1.6: The universal phase diagram of high-T_c cuprates (see text).

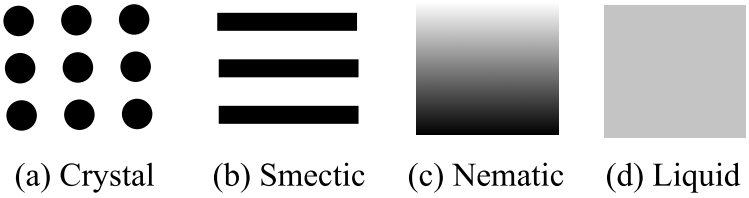

Figure 1.7: Successive restoration of space symmetries, as a melting of (a) crystal. Electronic example are localized electrons of the Mott insulator. (b) The smectic phase has restored continuous translational symmetry horizontally. For electrons, this happens in a density wave. (c) The nematic phase has only rotational symmetry broken. Example with electrons is the Pomeranchuk instability. (d) The liquid has all continuous symmetries of space, i.e. the Euclid group. Fermi liquid is an electronic example.

The first such symmetry breaking example (Fig. 1.7) in cuprates were "stripes", a special type of a charge density wave (CDW). They were first derived from the consideration of Hubbard model [93]. The physical picture is of the doped holes trying to gain kinetic energy, without disrupting the existing antiferromagnetic order. Since this is impossible in $2d$, an optimal state is when holes delocalize along $1d$, forming stripes, while preserving the frozen spin ordering between them. The experimental verification arrived through measurement of spin ordering by neutron scattering: both static stripes [94–97], and indications of fluctuating, dynamical stripes [98] are observed. Local spectroscopic

measurements [99] corroborated this picture.An attempt at describing the phase diagram in view of stripe ordering first lead to the theory of an electronic liquid crystal [35, 100–102]. Although the situation is complicated by (chemical) disorder, the picture is a quantum mechanical version of the classical liquid crystal physics (see Fig. 1.7). The (bosonized) electronic crystal melts successively, forming stripes, which fluctuate and melt, leaving a nematic that finally disorders into a liquid. The superconductivity appears with appearance of liquid behavior.

The validity of this particular overarching liquid crystal picture is still open to experimental confirmations, but the general view on electrons breaking the lattice symmetry has gotten additional recent vindication. Charge and heat transport measurements [103, 104], neutron scattering [105], as well as atomic resolution spectroscopic STM measurements [99,106], have shown a transition to an electronic nematic state (Fig. 1.7), that seems to coincide with the transition to the pseudogap phase.

Our motivation for Chapter 7 is a field theory based analysis of the coexistence of various symmetry breaking patterns found in the STM measurements on underdoped cuprates. In Chapter 6 we will focus on stripes only, and consider the temperature dependent effect of this ordering on the optical phonons of the crystal.

1.4 This thesis

The recurring theme of this thesis is the topological effect of dislocations. There are however two parts of the thesis, in which the principal role of the defect differs. In the first part, comprised of Chapters 2, 3, 4, 5, the motivation is the uncovering of the topological translational effect of lattice dislocations on fermionic Dirac particles which appear in the effective theories of graphene and topological insulators. In the second part, the defects appear in form of stripe dislocations in underdoped cuprates, and turn out to play a major role for the bosonic order parameters which describe the electronic charge degree of freedom. Finally, Chapter 6 stands out in the sense that no topological defects are considered within it, but instead the coupling of the particular bosonic order parameter of cuprates, the stripes, to the lattice phonons is analyzed.

Chapter 2 uncovers a direct connection between gravitating Dirac fermions, and graphene electrons in presence of lattice topological defects. The lifting of the lattice elasticity/gravity correspondence into the arena of electrons has entered a new realm since the appearance of graphene Dirac electrons. The fundamental theory of gravitating fermions is in principal richer than the one of scalars, because of the more manifest presence of torsion. Torsion is related to the local translational properties of the curved spacetime, and although might be small for the fundamental interactions, becomes fully exposed in the lattice setting. We expand (and reinterpret) previous attempts at describing disclinations in graphene as curvature sources, by including dislocations as torsion sources. This

fundamental step helps clarifying the role of the lattice for the graphene Dirac particles: We can show that the rotational and translational actions on the Dirac spinors, coming from the fundamental curvature and torsion, can be directly mapped onto the defected graphene lattice version, by extending the generators of the Euclid group. The result shows that the lattice fermion doubling, which produces the two graphene valleys separated by the inverse lattice constant $1/a$, can also be viewed as a modification of the Euclid space group generators by corrections proportional to a. The uncovered space group of the defected lattice signals the non-trivial exchange statistics of the defects, as experienced by the Dirac particles.

In Chapter 3 we continue by considering the experimental observation of the topological effect of dislocations on graphene electrons. The topological effect is represented by the holonomy (the Berry phase) of the electron upon encircling a defect, which is a quantized quantity. An Aharonov-Bohm type interferometer presents itself as the natural experimental setup. Quite surprisingly, we find that the translational holonomy caused by the Burgers vector is deeply related to a singular behavior, where the Onsager transport symmetry can be violated at mesoscopic scales. The experimental realization of the proposed interferometer, and the test of the fundamental effect, is becoming feasible in the near future.

The essence of the effect lies in two concurring properties: (i) That the topological dislocation holonomy acts as an effective Aharonov-Bohm magnetic field (of opposite sign) in each graphene valley, and (ii) The possibility to spatially separate the points in the device, where the equilibration of valleys occurs. The two graphene valleys are connected by time reversal (hence the opposite sign of the effective magnetic field of dislocation). When a finite dephasing length spans the device size, but is not much longer, the spatial separation of points in the device where the intervalley scattering occurs, prohibits the coherent equilibriation of the two valleys. In the absence of equal coherent contributions of the two valleys, the dislocation effective fields of opposite sign cannot cancel, and a total Aharonov-Bohm phase adds to the true magnetic field. This appears as an uneven magnetoconductance, prohibited in systems with time reversal symmetry by Onsager relations. The predicted singular behavior due to intrinsically non-equilibriated current flowing dominantly in one valley is a strong test of our understanding of dephasing and the transition between the quantum mechanical and classical behavior.

In Chapter 4 we descend our description to the defect core of dislocations, finding the precise relation between the lattice and continuum descriptions of the defect. The study is of direct relevance to the recent atomically resolved STM measurements of graphite surfaces with grain boundaries. The grain boundaries can be represented as arrays of dislocations, and we therefore dedicate this Chapter to the interpretation of the STM measurement of the local density of states (LDOS) near the defects. One of the peculiar observations is the appearance of LDOS enhancement at zero energy. We find that the continuum field theory allows for two types of microscopic completions (self-adjoint extensions), where

one hosts zero energy localized states at the defect core, and the other does not. These two physical realizations we identify with two inequivalent stable microscopic atom arrangements of the defect core in a tight binding lattice calculation of the LDOS. This suggests an explanation of found zero modes in terms of the exact core structure, and an accompanying completion of the continuum theory.

The experiments however show different LDOS behavior for large- and small-angle grain boundaries. Since the former cannot always be described as arrays of simple dislocations, we also simulate tight-binding amorphous grain boundaries in graphene (i.e. the graphite surface). These grain boundaries are strongly disordered, but still allow for a distinction between the case of forming a 1d band with van Hove singularities in the LDOS (large angle), and the case of single peak LDOS enhancements near zero energy (small angle).

Chapter 5 is dedicated to an analysis of crystal dislocations in a topological insulator (TI). Recent results showed that these defects in 3d TIs host zero modes of fermionic nature. We however consider a more elementary setup, of a 2d TI pierced through by the dislocation lines of the hosting 3d crystal. The edge of this 2d TI carries (for simplicity) a single pair of propagating modes that have opposite helicity. A well-known fact is that, if one shapes the 2d TI into an interferometer, a piercing magnetic field would cause a persistent current on the edge. The dislocation however respects time reversal symmetry, and therefore induces the opposite boundary conditions on the two edge wavefunctions: the two edge modes are both set in motion equally, so that the total charge current vanishes (as it must). However, this motion corresponds to a net spin current! We find that the production of the simple excitation in form of the spin current by the dislocations, raises questions about the deep connection of the topological defect to the topological bulk.

In Chapter 5 however we focus on a useful side product of the induced spin current (which by itself would be harder to measure). Namely, the edge of the 2d TI can host localized Majorana fermionic bound states, and these are proving important in the raising field of quantum computation. Even if they would successfully be produced on the 2d TI edge today, one finds that their detection by an Aharonov-Bohm interference is obstructed by the fact that their effect obeys a spin-flip symmetry. The dislocation induces spin current on the other hand, breaks this symmetry, and allows for the signatures of the Majorana states to the appear in the conductance of the interferometer. We hope these findings will stimulate experimental efforts in manipulating dislocations via crystal strains, and using them as novel probes in interferometry.

In Chapter 6 we consider the coupling of stripes to the optical phonons of the cuprate perovskite plane. The stripes represent charge density waves (CDW), and we assume the static metallic stripe ordering. The peculiar nature of the 1d system of electrons living on the stripes leads to very specific predictions, and several *a posteriori* explanations of existing experiments. The phonon anomaly wavevector is parallel to the stripes, and the anomaly energy width shrinks with raising temperature, as observed in measurements. A specific doping dependence,

and additional structures in the phonon spectral function are predicted. All these features follow the fact that the phonon anomaly is connected to the on-stripe density fluctuations of the quasi-1d electron system, and not to the transversal stripe fluctuations, as was assumed in previous models. Since this Chapter deals with the nature of cuprate stripes in some detail, it also serves as an introductory step for the dealing with stripe dynamics, which is part of the subject of Chapter 7.

The final Chapter 7 of this thesis is dedicated to a theoretical analysis of recent STM results on underdoped cuprates. We focus on the electronic liquid crystalline aspects of these strongly correlated systems, as it is widely expected that the local crystal symmetry breaking is relevant for both the pseudogap phase, and the superconductivity. We begin by Fourier analysis of the real space atomic resolution STM data. We can define a local nematic order parameter by looking at the asymmetry between the x and y Bragg peaks of the lattice periodicity. At the same time, the Fourier data around $3/4a$ peaks in the BZ reveals the characteristic $4a$ period order, i.e. the stripes. The energy dependence of the STM measurement can be changed, and the evolution of these orderings as the pseudogap energy scale is reached can be assessed.

From the data, it seems that the correlation length of the stripe CDW stays short at all energies. We find that the CDW (stripe) phase is also very disordered, giving strong evidence that the stripes form an incommensurate CDW in these underdoped cuprates. We make an even stronger statement: the disorder in the phase of the stripes is determined by the appearance of stripe dislocations and anti-dislocations! These are defects in which the stripe phase has a non-vanishing winding, so that a stripe line ends inside the field of view. The role of these topological defects is therefore obviously important, and there are indications they might be locally connected to the dopant oxygen sites (external disorder).

Our goal is however to understand the more complete liquid crystal picture, and there we find a big surprise. Namely, one would expect that the melting of the stripes (which represent smectic order) by the topological defects is correlated with the appearance of nematic ordering. We however find that these two are not related! Instead the nematic order develops an expectation value (the correlation length spans the finite field of view), while no related change of the stripes or relation to the stripe dislocations is found. The two seem independent at this level. This suggests that the nematic ordering as defined by the Bragg peaks (i.e. an intra-unit-cell nematic ordering) is maybe not the nematicity related to the stripe melting.

We continue by constructing a Ginzburg-Landau field theory for the smectic and nematic orderings and their coupling. This coupling is at the level of local nematic fluctuations, because the nematic order itself turned out to be insensitive to the stripes. We find that in the intra-unit-cell nematic phase, the coupling which is linear in the stripe phase and in the nematic fluctutation is the most important. This coupling contains the characteristic stripe dislocation singularities in the phase of the stripe CDW. It induces a dipole shaped fluctuation in

the nematic order, so that the dislocation is at the boundary between opposite signed nematic fluctuation regions — this relationship is exactly observed in the experimental STM data.